DOK3 promotes proliferation and inhibits apoptosis of prostate cancer via the NF-κB signaling pathway

Kun Jin[1], Shi Qiu[2], Bo Chen[3], Zilong Zhang[1], Chichen Zhang[1], Xianghong Zhou[1], Lu Yang[1], Jianzhong Ai[3], Qiang Wei[1]

[1]Department of Urology and National Clinical Research Center for Geriatrics, West China Hospital, Sichuan University, Chengdu, Sichuan 610041, China;
[2]Center of Biomedical Big Data, West China Hospital, Sichuan University, Chengdu, Sichuan 610041, China;
[3]Department of Urology and Institute of Urology, West China Hospital, Sichuan University, Chengdu, Sichuan 610041, China.

Abstract

Background: DOK3 (Downstream of kinase 3) is involved primarily with immune cell infiltration. Recent research reported the role of DOK3 in tumor progression, with opposite effects in lung cancer and gliomas; however, its role in prostate cancer (PCa) remains elusive. This study aimed to explore the role of DOK3 in PCa and to determine the mechanisms involved.

Methods: To investigate the functions and mechanisms of DOK3 in PCa, we performed bioinformatic and biofunctional analyses. Samples from patients with PCa were collected from West China Hospital, and 46 were selected for the final correlation analysis. A lentivirus-based short hairpin ribonucleic acid (shRNA) carrier was established for silencing DOK3. A series of experiments involving the cell counting kit-8, bromodeoxyuridine, and flow cytometry assays were performed to identify cell proliferation and apoptosis. Changes in biomarkers from the nuclear factor kappa B (NF-κB) signaling pathway were detected to verify the relationship between DOK3 and the NF-κB pathway. A subcutaneous xenograft mouse model was performed to examine phenotypes after knocking down DOK3 *in vivo*. Rescue experiments with DOK3 knockdown and NF-κB pathway activation were designed to verify regulating effects.

Results: DOK3 was up-regulated in PCa cell lines and tissues. In addition, a high level of DOK3 was predictive of higher pathological stages and worse prognoses. Similar results were observed with PCa patient samples. After silencing DOK3 in PCa cell lines 22RV1 and PC3, cell proliferation was significantly inhibited while apoptosis was promoted. Gene set enrichment analysis revealed that DOK3 function was enriched in the NF-κB pathway. Mechanism experiments determined that knockdown of DOK3 suppressed activation of the NF-κB pathway, increased the expressions of B-cell lymphoma-2 like 11 (BIM) and B-cell lymphoma-2 associated X (BAX), and decreased the expression of phosphorylated-P65 and X-linked inhibitor of apoptosis (XIAP). In the rescue experiments, pharmacological activation of NF-κB by tumor necrosis factor-α (TNF-α) partially recovered cell proliferation after the knockdown of DOK3.

Conclusion: Our findings suggest that overexpression of DOK3 promotes PCa progression by activating the NF-κB signaling pathway.

Keywords: Prostate cancer; Downstream of kinase 3; Prognosis; Nuclear factor kappa B

Introduction

As the most common malignancy in males, prostate cancer (PCa) is estimated to have 248,530 new cases and is the second leading cause of cancer deaths in the United States in 2021.[1] Recently, patient survival has benefited from developments in screening methods and treatments.[2-4] However, despite receiving adequate therapies, some patients may experience recurrence, progression, or even metastasis.[5] Therefore, recognizing potential progression biomarkers and identifying novel therapeutic targets may improve our understanding of the mechanisms involved in PCa and promote better clinical decision-making when it comes to treatment.

There are many studies explaining the possible mechanisms of PCa progression. Several investigations revealed a potential link between chronic inflammation and PCa,[6-8] indicating that the inflammatory microenvironment could regulate progression. Others reported that cancer stem cells, with a capacity for self-renewal and proliferation, play an essential role in tumor growth, thus causing resistance to radiation, androgen deprivation therapy, and chemotherapy in patients with PCa.[9,10] In addition, a group of studies focusing on the immune-related microenvironment reported that both innate and adaptive immune cells contribute to PCa progression.[11] As an immunogenic disease, PCa could evade the immune

Access this article online

Quick Response Code:

Website: www.cmj.org

DOI: 10.1097/CM9.0000000000002251

Kun Jin, Bo Chen, and Shi Qiu contributed equally to this work.

Correspondence to: Dr. Qiang Wei, Department of Urology, Institute of Urology, West China Hospital, Sichuan University, No. 37 Guoxue Alley, Chengdu, Sichuan 610000, China
E-Mail: wq933@hotmail.com

Chinese Medical Journal 2023;136(4)
Received: 05-05-2022; **Online:** 02-03-2023 **Edited by:** Yuanyuan Ji

system by inducing T-cell apoptosis, thus causing ineffective antigen presentation.[12,13] Although various mechanisms have been considered, the exact etiology of PCa remains unknown.

DOK (Downstream of kinase) is a family of adaptor proteins that act as catalysts by connecting protein tyrosine kinases and their downstream effectors.[14] As a member of the DOK family, DOK3, binding the cytoplasmic protein tyrosine kinases Abl, was first discovered by Cong *et al*[15]. Since DOK3 is an adaptor, it can bind molecules, thus participating in various intracellular signal transduction processes, especially signaling the B cell receptor in B cells and other innate immune cells.[16-22] Liu *et al*[23] reported that DOK3 negatively regulated inflammatory cell infiltration and the generation of inflammatory cytokines, thereby suppressing acute respiratory distress syndrome induced with lipopolysaccharides in mice. In two studies that focused on the effects of DOK3 on tumors, one showed that overexpression of DOK3 indicated high suppressive immune cell infiltration, leading to a worse prognosis for gliomas;[24] the other study performed by Berger *et al*[25] found that DOK3 was a lung tumor suppressor, while combined loss of DOK1, DOK2, and DOK3 enhanced neoplastic transformation. These two studies reported opposite effects of DOK3 on tumor promotion and no relevant exploration of PCa; therefore, we aimed to investigate the role of DOK3 in PCa progression.

Methods

Ethical approval

The study was conducted in accordance with the *Declaration of Helsinki* and was approved by the Institutional Ethics Review Board of West China Hospital of Sichuan University (No. 2017-324). Informed written consent was obtained from all patients before enrollment in this study.

Patient samples

A total of 46 human PCa specimens were acquired from the Department of Urology at West China Hospital, Sichuan University, following radical prostatectomy. Patients with other types of cancer or a previous surgical history were excluded. Pathological characteristics, including tumor (T) stage and Gleason score (GS), were collected.

Cell lines and cell culture

Human PCa cell lines (22RV1, LNCAP, DU145, and PC3) and the prostate epithelial cell line HPEPic (RWPE-1) were purchased from the American Type Culture Collection (Rockville, MD, USA). Normal prostate epithelium cells were incubated in Prostate Epithelial Cell Medium (ScienCell Research Laboratories, Inc., Carlsbad, CA, USA), while all PCa cell lines were cultured with RPMI-1640 medium (HyClone Laboratories, Inc., Logan, UT, USA). Additions to the medium used for PCa cell culture included 10% fetal bovine serum (Gibco, NY, USA), penicillin 100 U/mL, and streptomycin 100 μg/mL (Invitrogen, Carlsbad, CA, USA). All cell lines were incubated in a humidified atmosphere with 5% CO_2 at 37°C.

Quantitative real-time PCR analysis

All ribonucleic acids (RNAs) were extracted from cell lines using Trizol reagent (Invitrogen) according to the manufacturer's instructions. A PrimeScript RT reagent kit (Takara, Dalian, China) was used for reverse transcription. The quantitative real-time polymerase chain reaction (qRT-PCR) assays were performed using SYBR Green with ABI Prism 7300 SDS software (Thermo Fisher Scientific, Waltham, USA) to examine gene expression levels. The cycle numbers of the target genes were normalized based on those of glyceraldehyde-3-phosphate dehydrogenase (GAPDH) to obtain a ΔCT value. The calculation equation of relative messenger ribonucleic acid (mRNA) level was $2^{-\Delta\Delta CT}$.

The primer sequences for DOK3 were:

forward (F), 5′-CGGCTCCGACAAGATACTTC-3′ and reverse (R), 5′-TAGGCACGCAGCAAACTC-3′.

The primer sequences for GAPDH were:
F, 5′-AATCCCATCACCATCTTC-3′ and R, 5′-AGGCT GTTGTCATACTTC-3′.

Western blotting

Protein levels were estimated by Western blotting assays. Total protein of cell lines was obtained with a RIPA kit (Beyotime, Shanghai, China). Using the bicinchoninicacid Protein Assay Kit (Beyotime, Shanghai, China), the protein concentration of each sample was measured. Denatured cellular protein lysates were separated on a 10% sodium dodecyl sulfate-polyacrylamide gel and electro-transferred to a polyvinylidene fluoride membrane (Millipore, Billerica, MA, USA). Membranes were blocked in 5% milk at room temperature for 1 h and incubated with primary antibodies overnight at 4°C. After three washes, membranes were incubated for 1 h at room temperature with goat anti-rabbit IgG or anti-mouse IgG (1:1000; Beyotime, Shanghai, China) as a secondary antibody. Protein bands were visualized using an enhanced chemiluminescent reagent (Millipore, Billerica, MA, USA). All primary antibodies, including DOK3 (1:1000), P65 (1:1000), phosphorylated-P65 (p-P65) (1:1000), B-cell lymphoma-2 like 11 (BIM) (1:1000), B-cell lymphoma-2 associated X (BAX) (1:1000), X-linked inhibitor of apoptosis (XIAP) (1:1000), and β-actin (1:1000) were purchased from Abcam (Abcam, Cambridge, England).

Knockdown of DOK3

The lentivirus construction of DOK3 knockdown was designed and synthesized by SyngenTech (Beijing, China). Specific short hairpin RNA (shRNA) sequences were:

shDOK3-1, F, 5′-CCGGTTCTACCAGCAGCATGTCA ACTCGAGTTGACATGCTGCTGGTAGATTTTTG-3′ and R, 5′-AATTCAAAAATCTACCAGCAGCATGTCAA CTCGAGTTGACATGCTGCTGGTAGAA-3′; shDOK3-

2, F, 5′-CCGGTTCCTCTACCAGCAGCATGTCTCGAGACATGCTGCTGGTAGAGGATTTTTG-3′ and R, 5′-AATTCAAAAATCCTCTACCAGCAGCATGTCTCGAGACATGCTGCTGGTAGAGGAA-3′. PCa cells were plated in 6-well dishes and infected with DOK3 knockdown lentivirus (shDOK3-1, shDOK3-2) in 22Rv1 and PC3 cells. Pools of stable transductions were generated by selection using puromycin (2 μg/mL) for 2 weeks.

Cell proliferation assay

Cells were seeded in 96-well plates at a density of 5×10^3 cells/well, and cell viability was measured by cell counting kit-8 (CCK-8) assays for 12, 24, 48, and 72 h. Subsequently, CCK-8 solution (US Everbright, California, USA) was added at 10 μL/well, and the absorbance was measured at a wavelength of 450 nm after incubation for 2 h.

Bromodeoxyuridine (BrdU) assay

The BrdU assay (GENMED, Boston, US) was performed to measure cell proliferation. In brief, ~2×10^6 cells were seeded in a 60-mm culture plate containing a glass slide. After adherence to the slide, cells were successively labeled, washed, immobilized, blocked, and stained according to the manufacturer's instructions. The glass slide was combined with anti-photochemical quenching and mounted, and then examined using an inverted fluorescence microscope (Olympus; Tokyo, Japan).

Apoptosis assay

After separating the media, cells were digested with EDTA-free trypsin, centrifuged (2000 ×*g* for 5 min), and washed twice with cold phosphate-buffered saline (PBS). Following centrifugation at the same rate, cells were resuspended in 100 μL of buffer, consisting of 5 μL of propidium iodide and 5 μL of fluorescein isothiocyanate-labeled Annexin V (BD Biosciences, New Jersey, USA). After incubation in the dark for 15 min at room temperature, the proportion of apoptotic cells was detected by flow cytometry.

Xenografts in mice

The animal experiments were approved by the ethics committee of West China Hospital of Sichuan University, and all animal procedures were carried out in compliance with the Guidelines for the Care and Treatment of Laboratory Animals. Twelve BALB/c male nude mice (4–6 weeks old) were purchased from Shanghai SLAC Laboratory Animal Co. (Shanghai, China) and randomly divided into two groups: shDOK3 ($n = 6$) and negative control ($n = 6$). Approximately 5×10^6 22RV1 cells which stably expressed shDOK3 or control shRNA were injected into the left flank of each mouse. Tumor measurements were performed every 3 days after macroscopic tumor appearance and were calculated according to the following formula: $V = 0.5 \times \text{length} \times \text{width}^2$. Three weeks later, the mice were euthanized, and the tumors were removed to measure and photograph.

Histology and immunofluorescence

The tumor tissues were fixed in 4% paraformaldehyde, embedded in paraffin, and sectioned for further hematoxylin and eosin staining and immunofluorescence. Tissue sections were deparaffinized in xylene twice for 10 min and rehydrated in a series of alcohols with different concentrations (95%, 80%, and 75% for 5 min each). After antigen retrieval using citrate buffer in an autoclave, endogenous peroxidase activity was blocked using 0.5% H_2O_2. Following three washes with PBS, the glass slides were incubated with primary antibody (anti-Ki67 antibody/anti-proliferating cell nuclear antigen [PCNA] antibody, Abcam; Cambridge, MA, USA) overnight at 4°C. The next day, a corresponding secondary antibody with fluorescence was added at 37°C for incubation. Nuclei were stained with 4′, 6-diamidino-2-phenylindole. Images were acquired using an Olympus inverted fluorescence microscope.

Immunohistochemistry

Tumor tissue sections were paraffin-embedded, deparaffinized with xylene, and rehydrated with ethanol of gradient concentrations. Antigen retrieval was performed using citrate buffer in a water bath kettle. All sections were then incubated with H_2O_2 and blocked with normal goat serum. After washing with PBS, an anti-DOK3 antibody was added dropwise to all sections and incubated at 4°C overnight. The next day, a secondary antibody was added after three washes with PBS. Chromogenic detection was performed using diaminobenzidine, and slides were then counterstained with hematoxylin. After dehydration and mounting, images were captured using an Olympus microscope (Tokyo, Japan). Quantitative analyses were performed by combining the area percent of positive neurons and the relative intensity of the staining gray level.

Statistical analysis

RNA-seq data of prostate cancer were downloaded from The Cancer Genome Atlas project (TCGA, http://portal.gdc.cancer.gov). Samples were obtained and processed according to protocols from National Cancer Institute's Biospecimen Research Database (https://brd.nci.nih.gov/brd/). All genes were transformed into a gene symbol matrix using Ensembl ID data from the Ensembl database (http://asia.ensembl.org/index.html). Clinicopathological features and survival outcomes were extracted and combined with this data.

First, the expression level of DOK3 was evaluated in tumor samples compared with normal tissues. Unpaired *t*-tests were performed to evaluate the differences between the two groups (normal tissue *vs*. tumor tissue). Second, clinicopathological features were extracted and analyzed combined with the DOK3 expression level. For multiple comparisons, a chi-squared test was applied for normal distribution data, while a Kruskal-Wallis test was applied for abnormal distribution data. Third, the Kaplan-Meier method was applied for survival analysis, and the survival rate between the two groups was compared using a log-rank test. Gene set enrichment analysis (GSEA) was

carried out using the GSVA R package v1.30.0 (http://www.gsea-misgdb.org/gsea/index.jsp). After collecting gene sets for epithelial-mesenchymal transition, stem cell, proliferation, and cell cycle-related pathways, the enrichment score for each sample was obtained using the gene expression profile. R 3.6.3 (https://cran.r-project.org) and GraphPad Prism 8.0 software (GraphPad Software, California, USA) was used for statistical analysis. For all analyses, $P < 0.05$ was considered statistically significant.

Results

DOK3 was up-regulated in PCa and correlated with patient prognoses

To evaluate the role of DOK3 in PCa, we used sequencing data and corresponding clinical data from the TCGA database to perform a series of analyses. According to the differential expression analysis, a higher expression level of DOK3 was observed in PCa tissues ($n = 52$) compared with normal prostate tissues ($n = 499$) [Figure 1A]. Furthermore, we detected a relationship between DOK3 expression level and clinicopathologic features, finding that a higher DOK3 expression level was associated with a higher T stage, N stage, and GS [Figure 1B–D]. We hypothesized that DOK3 might play an important role in PCa growth and progression, so we performed overall survival and biochemical recurrence-free survival analysis. As expected, a worse prognosis was observed in the DOK3 high expression level group [Figure 1E and F]. To verify these results, we performed qRT-PCR and Western blotting assays to detect the expression level of DOK3 *in vitro*. As anticipated, higher DOK3 expression was observed in human PCa cell lines, in which 22RV1 showed the highest expression level [Figure 1G and H].

Expression of DOK3 positively correlated with higher GSs in human tissues

Although we observed a higher expression level of DOK3 in the PCa cell line, we wondered whether results in human tissues would be similar; therefore, we performed an immunohistochemistry assay, evaluating both the proportion of positive areas and relative intensity. Characteristics of patients ($N = 46$) are shown in Table 1 and Supplementary Table 1, http://links.lww.com/CM9/B295. Quantification of these two indicators using corresponding scores revealed a significant correlation between the DOK3 expression level and the GS. A higher DOK3 expression level was associated with a higher GS ($P = 0.021$) [Figure 2A and B]. However, no significance was found in the correlation analysis of DOK3 expression and pathological T stage ($P = 0.695$) [Figure 2C and D]. These results indicate that DOK3 possibly promotes PCa cell growth and further mediates its poor differentiation.

DOK3 knockdown inhibited cell proliferation and promoted apoptosis of PCa cells

Since we found higher DOK3 levels in PCa cell lines and a potential role in PCa growth, we next evaluated whether down-regulating DOK3 through external intervention could affect the growth process. To assess knockdown efficiency, we performed a qRT-PCR assay, which showed

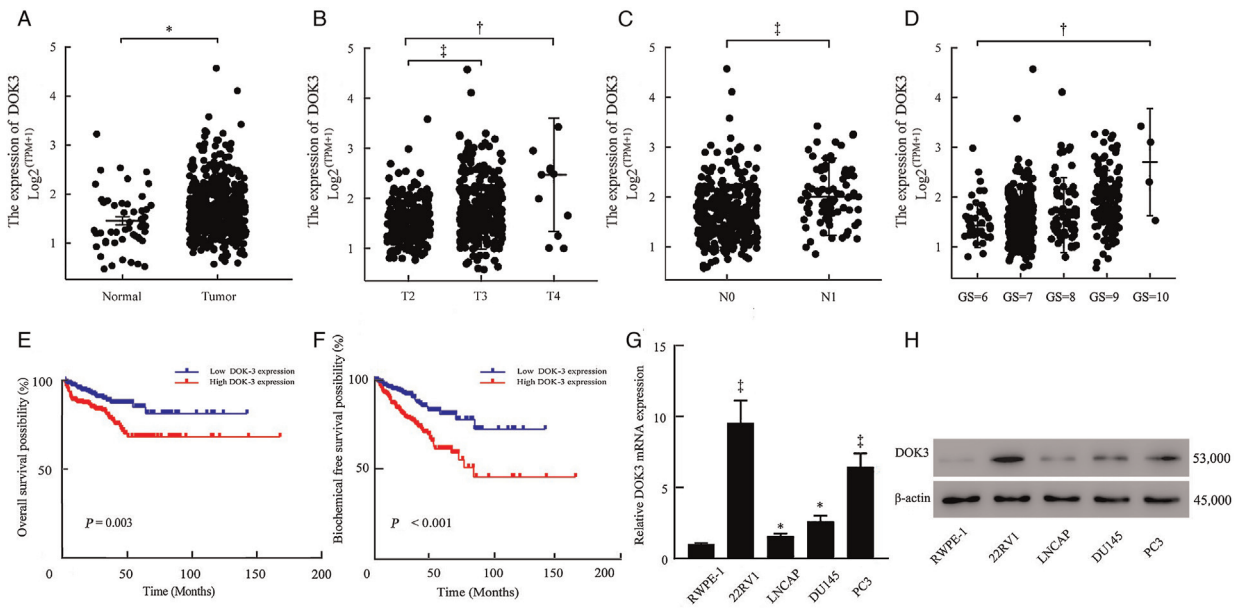

Figure 1: DOK3 is overexpressed in human PCa tissues and cultured PCa cells. (A) The expression level of DOK3 in the comparison between tumor tissues and normal prostate tissues (TCGA data, tumor tissue, $n = 52$; normal tissue, $n = 499$) (Wilcoxon rank sum test, $Z = 9641$, $P = 0.002$). (B–D) Correlation analyses of DOK3 expression and clinical characteristics including T stage (T2: $n = 189$; T3: $n = 292$; T4: $n = 11$) (Kruskal-Wallis Test, $H = 26.024$, $P < 0.001$), N stage (N0: $n = 347$; N1: $n = 79$) (Wilcoxon rank sum test, $Z = 8397$, $P < 0.001$), and GS (GS = 6, $n = 46$; GS = 7, $n = 247$; GS = 8, $n = 64$; GS = 9, $n = 138$; GS = 10, $n = 4$), respectively (TCGA data) (Kruskal-Wallis Test, $H = 40.524$, $P < 0.001$). (E, F) Survival analysis of overall survival outcomes (Log rank test, $X^2 = 8.985$, $P = 0.003$) and biochemical free survival outcomes (Log rank test, $X^2 = 17.35$, $P < 0.001$) after dividing into two groups according to the expression level of DOK3, measured by Kaplan-Meier method (TCGA data). (G, H) qRT-PCR assay and Western blotting assay assessing the mRNA and protein level of DOK3 in a normal prostate cell line and PCa cell lines. Data represent mean ± SD, $^{*}P < 0.01$, $^{\dagger}P < 0.05$, $^{\ddagger}P < 0.001$. DOK3: Downstream of kinase 3; GS: Gleason score; PCa: Prostate cancer; TCGA: The Cancer Genome Atlas project; T: Tumor (T) stage; N: N stage; qRT-PCR: quantitative real-time polymerase chain reaction; SD: Standard deviation.

Table 1: Characteristics of PCa patients involved in IHC assay ($N = 46$).

Characteristics	Values
Age (years), mean ± SD	70.3 ± 7.2
BMI (kg/m^2), mean ± SD	23.96 ± 2.61
PSA (ng/mL), median (Q1–Q3)	20.24 (11.97–32.62)
Pathology T stage, *n* (%)	
T2b	4 (9)
T2c	17 (38)
T3b	10 (22)
T3c	11 (24)
T4	3 (7)
Pathology GS*, *n* (%)	
7	23 (51)
8	4 (9)
9	17 (38)
10	1 (2)
The ISUP grade*, *n* (%)	
2	7 (15)
3	17 (38)
4	4 (9)
5	17 (38)

*One patient received preoperative androgen depressed treatment and GS could not be evaluated, while one patient presented as pathology T2 stage and could not be divided into a corresponding subgroup. PCa: Prostate cancer; GS: Gleason score; IHC: Immunohistochemistry; ISUP: International Society of Urological Pathology; Q1: Quantile 1 (25%); Q3: Quantile 3 (75%); SD: Standard deviation; BMI: Body mass index; PSA: Prostate specific antigen; T: Tumor.

a significant decrease in the mRNA level of two DOK3 shRNAs [Figure 3A]. Correspondingly, Western blotting results presented the same trend, with both shRNAs reaching the lowest protein level [Figure 3B], further confirming the knockdown effect. Since a higher DOK3 level was associated with poor differentiation and poor survival outcomes, in theory, DOK3 knockdown might present a decline in tumor growth. Thus, we performed proliferation and apoptosis assays exploring the role of DOK3. In the CCK-8 assay, significantly slower growth rates were observed in two PCa cell lines after silencing DOK3 compared with the shNC group [Figure 3C]. In addition, we performed the BrdU assay to examine cell proliferation. Our results demonstrated a significant reduction in the rate of 22RV1 cell proliferation after DOK3 knockdown [Figure 3D]. In the cell apoptosis assay, the apoptosis rates were increased in cells with silenced DOK3 expression [Figure 3E]. In brief, all these results showed that silencing DOK3 could inhibit cell proliferation and, at the same time, promote cell apoptosis.

DOK3 regulated the NF-κB signaling pathway in PCa cell lines

After finding that changes in cell proliferation and apoptosis were associated with a decrease in DOK3 expression, we explored the mechanism of action of DOK3. Using two datasets, GSEA indicated a positive correlation between DOK3 and the NF-κB signaling pathway [Figure 4A and B]. Based on this finding, we measured the related protein expression level of this signaling pathway. Western blotting analysis showed that along with silencing DOK3, expressions of p-P65 and XIAP were decreased, while expressions of BIM and BAX were significantly increased [Figure 4C and D]. These results suggested that DOK3 might be associated with the NF-κB signaling pathway.

DOK3 knockdown inhibited tumor growth in vivo

To further identify the role of DOK3 in tumor growth, we constructed a xenograft model using nude mice. After successfully injecting 22RV1 cells, mice were fed under the same conditions for 12 days. According to tumor size measurements made every 3 days, we found limited tumor growth in the DOK3 knockdown group [Figure 5A and B], consistent with the *in vitro* results. At the end of the animal experiment, tumors were excised from the mice and processed onto histology slides. In the immunofluorescence assay, lower proportions of both Ki-67 and PCNA were observed in the DOK3 silenced group, reflecting the obstruction of proliferation [Figure 5C]. Additionally, Western blotting showed lower expression levels of Ki-67, PCNA, and p-P65 [Figure 5D], adding to the evidence that DOK3-mediated NF-κB activation promoted tumor growth *in vivo*.

The effect of silencing DOK3 was suppressed via activation of the NF-κB signaling pathway

To explore the functional association between DOK3 and the NF-κB pathway, we treated the DOK3 silenced group and the control group with TNF-α, an NF-κB pathway activator. Increased cell proliferation was observed [Figure 6A and B], and cell apoptosis weakened in the DOK3 silenced group [Figure 6C]. Additionally, biomarkers related to the NF-κB signaling pathway, such as p-P65 and XIAP, were up-regulated, while BIM and BAX were down-regulated [Figure 6D]. From these findings, we discovered that activation of the NF-κB pathway could reverse the effects of silencing DOK3. In conclusion, the tumor promotion role of DOK3 depended on activating the NF-κB pathway through increasing cell proliferation and decreasing apoptosis.

Discussion

DOK3 is abundantly expressed in hematopoietic cells, including B cells and macrophages, participating in various immunoreceptor signaling pathways.[14] In B cells, DOK3 plays both activating and inhibitory roles. On the one hand, DOK3 can accelerate plasma cell differentiation through regulating the expression of programed cell death 1 ligands,[18] while interacting with Grb2 and Cbl, facilitating B cell receptor-mediated antigen gathering.[26] On the other hand, DOK3 can not only inhibit the B cell receptor signaling pathway[14] and Ras-MAPK pathway,[15] also inhibit intracellular calcium signaling by combining Grb2.[20] As for macrophages, DOK3 mainly plays a negative role by inhibiting TLR4 signaling,[22,27] and decreasing IL-6 and TNF-α by inhibiting TLR9 signaling.[28] Related research has revealed that DOK3 has complex functions in other non-lymphoid cells, such as lung epithelial cells, osteoblasts, and osteoclasts.[25,29,30]

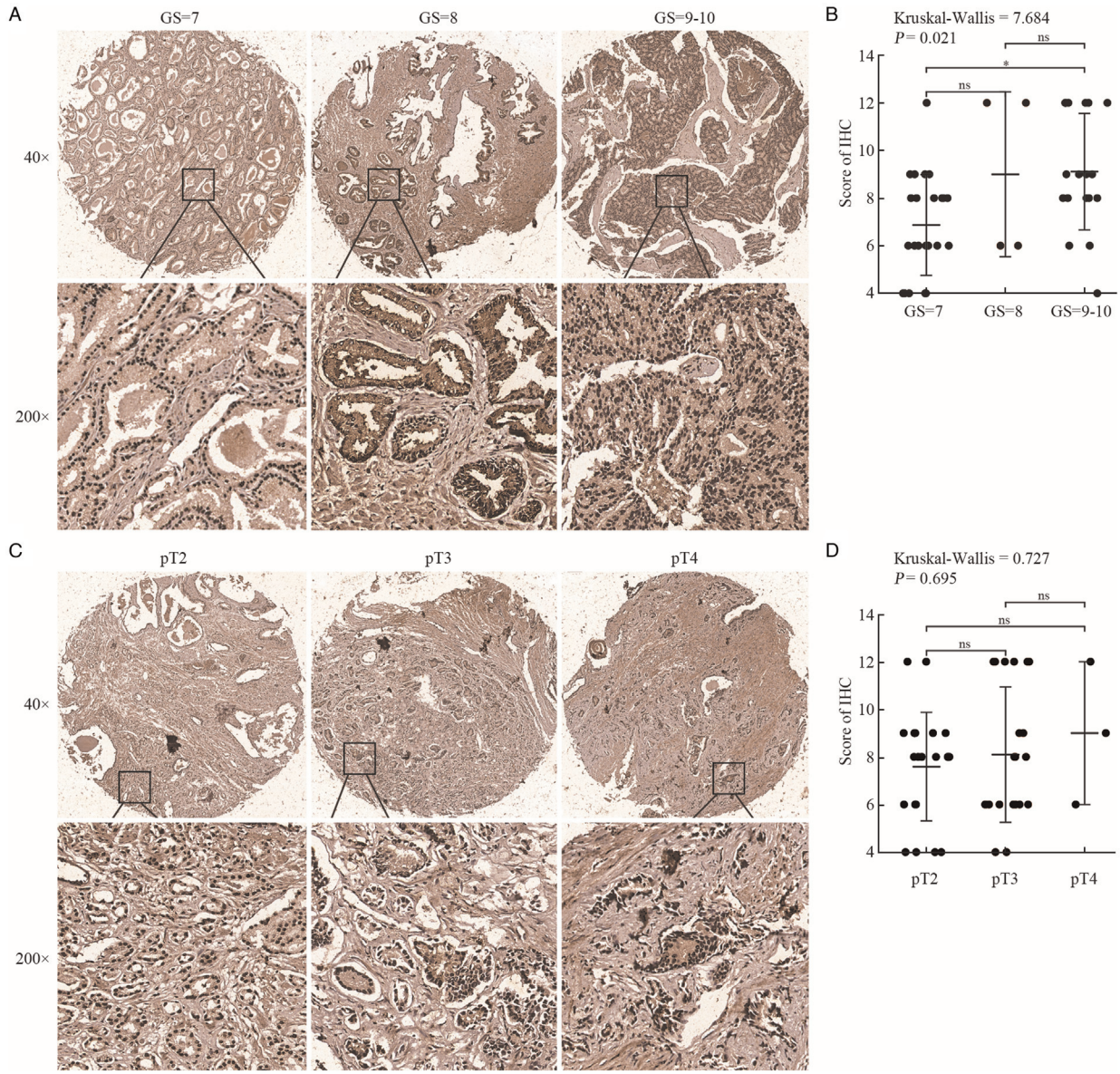

Figure 2: The expression of DOK3 was positively correlated with higher GS in human tissues. (A) Representative images of immunohistochemistry assay with distinctive GS, original magnification at 40 × and 200 × . (B) The correlation between IHC score and GS (GS = 7, $n = 23$; GS = 8, $n = 4$; GS = 9–10, $n = 18$) (One patient received neo-adjuvant ADT, leading to unmeasured GS). (C) Representative images of immunohistochemistry assay with distinctive pathological T stage, original magnification at 40 × and 200 × . (D) The correlation between IHC score and pT stage (pT2, $n = 22$; pT3, $n = 21$; pT4, $n = 3$). Data represent mean ± SD, $^{*}P < 0.05$. DOK3: Downstream of kinase 3; GS: Gleason score; IHC: Immunohistochemistry; pT: Pathological T stage; ns: No significant; SD: Standard deviation; ADT: Androgen deprivation therapy; T: Tumor stage.

Our study represents the first report of the effects of DOK3 in promoting PCa growth. According to survival analysis based on the TCGA database, a higher expression level of DOK3 indicated worse disease-specific and biochemical outcomes. In patient samples, a higher DOK3 level correlated with a higher GS. Using lentivirus-mediated shRNA in two PCa cell lines, growth was suppressed, and apoptosis was promoted. In the nude mouse xenograft model, DOK3 knockdown markedly decreased tumor growth. Taken together, these findings suggest DOK3 oncogenic activity in PCa.

Over the past decades, the NF-κB signaling pathway has been regarded as the central mediator of inflammation as well as a participant in innate and adaptive immune responses.[31] The NF-κB signaling pathway plays an essential role in various cellular processes, including inhibition of apoptosis[32-35] and stimulation of cell proliferation.[36]

In addition, NF-κB was activated by exposure to pro-inflammatory cytokines in the tumor microenvironment,[37] which revealed the importance of NF-κB in linking inflammation, immune response, and cancer development.[38]

Several studies mentioned a relationship between DOK3 and NF-κB. DOK3 knockout B cells exhibited greater induction of NF-κB, thus promoting stimulation of B cell receptors.[19] In neutrophils, DOK3 recruited Card9 and

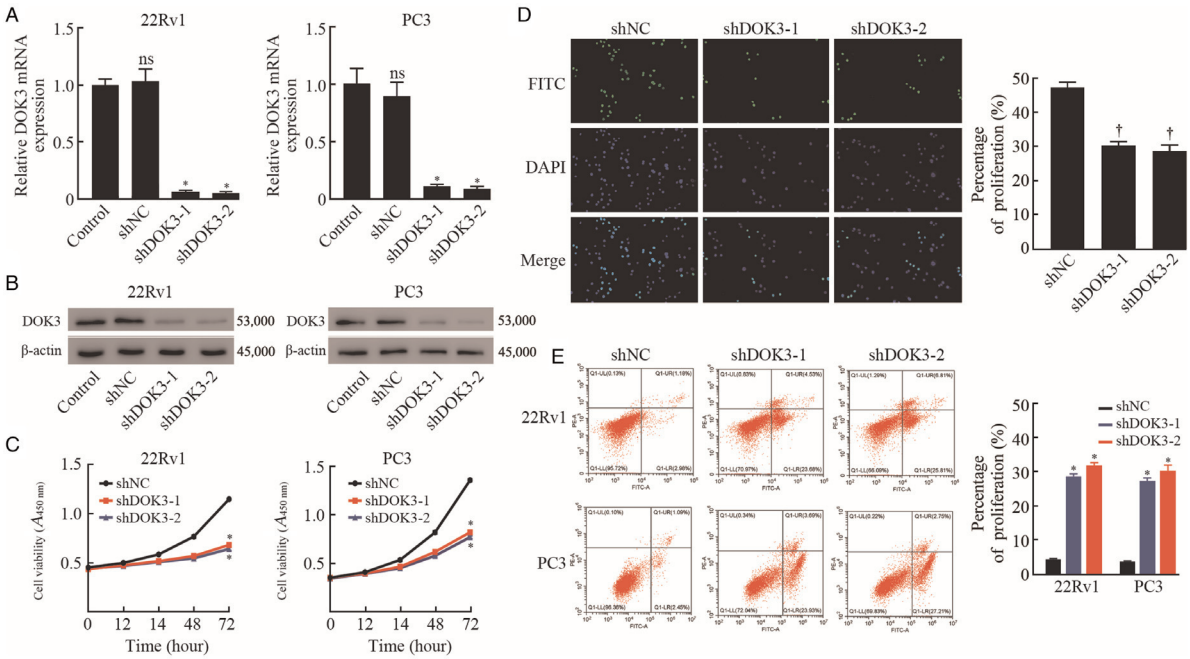

Figure 3: DOK3 knockdown suppresses the growth and promotes the apoptosis of cultured PCa cells. (A, B) qRT-PCR assay and Western blotting assay analyses of DOK3 in 22Rv1 (left panel) and PC3 (right panel) cells after transduction with shDOK3 *vs.* shNC lentivirus. (C) Cell viability of 22Rv1 and PC3 cells was determined using CCK-8 assay after transduction with shDOK3 *vs.* shNC lentivirus (Unpaired *t*-test). (D) Proliferative capacity of 22Rv1 cell line measured by BrdU assay. (E) Apoptosis rates were assessed after silencing DOK3 in two PCa cell lines measured by flow cytometry analysis. Data represent mean ± SD and Student's *t*-test was used. $^{*}P < 0.0001$, $^{\dagger}P < 0.001$. BrdU: Bromodeoxyuridine; CCK-8: Cell counting kit-8; DOK3: Downstream of kinase3; PCa: Prostate cancer; SD: Standard deviation; ns: No significant; shRNA: Short hairpin short hairpin ribonucleic acid; FITC: Fluorescein isothiocyanate; DAPI: 4',6-diamidino2-phenylindole; qRT-PCR: Quantitative real-time polymerase chain reaction.

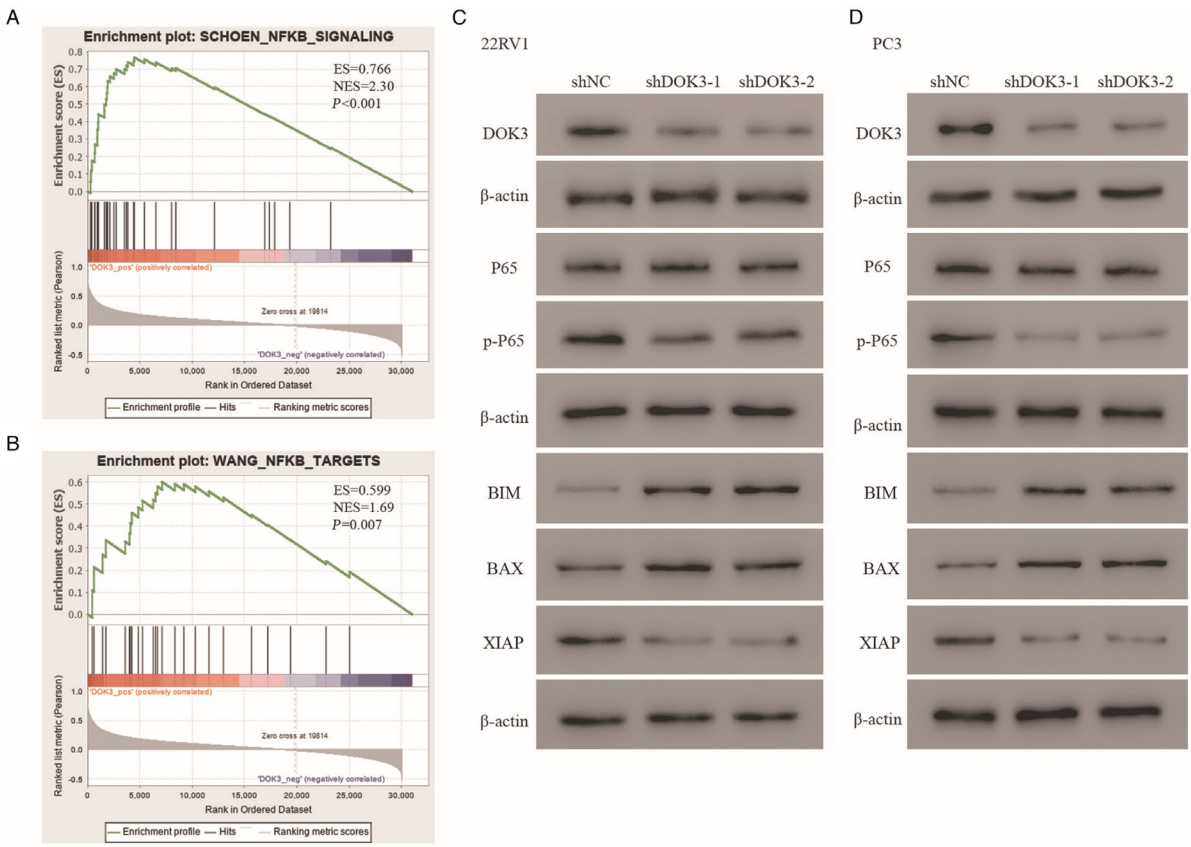

Figure 4: DOK3 knockdown suppresses the activation of NF-κB signaling pathway. (A, B) GSEA showing NF-κB targets are significantly enriched and correlated with DOK3. (C, D) Western blotting assays of p-P65, P65, BIM, BAX, and XIAP in 22Rv1 and PC3 cell lines with DOK3, shRNAs, or shNC RNA transfection, respectively. β-actin was used as the endogenous control for loading control. DOK3: Downstream of kinase 3; GSEA: Gene set enrichment analysis; NF-κB: nuclear factor kappa B; shRNA: Short hairpin RNA; p-P65: phosphorylated-p65.

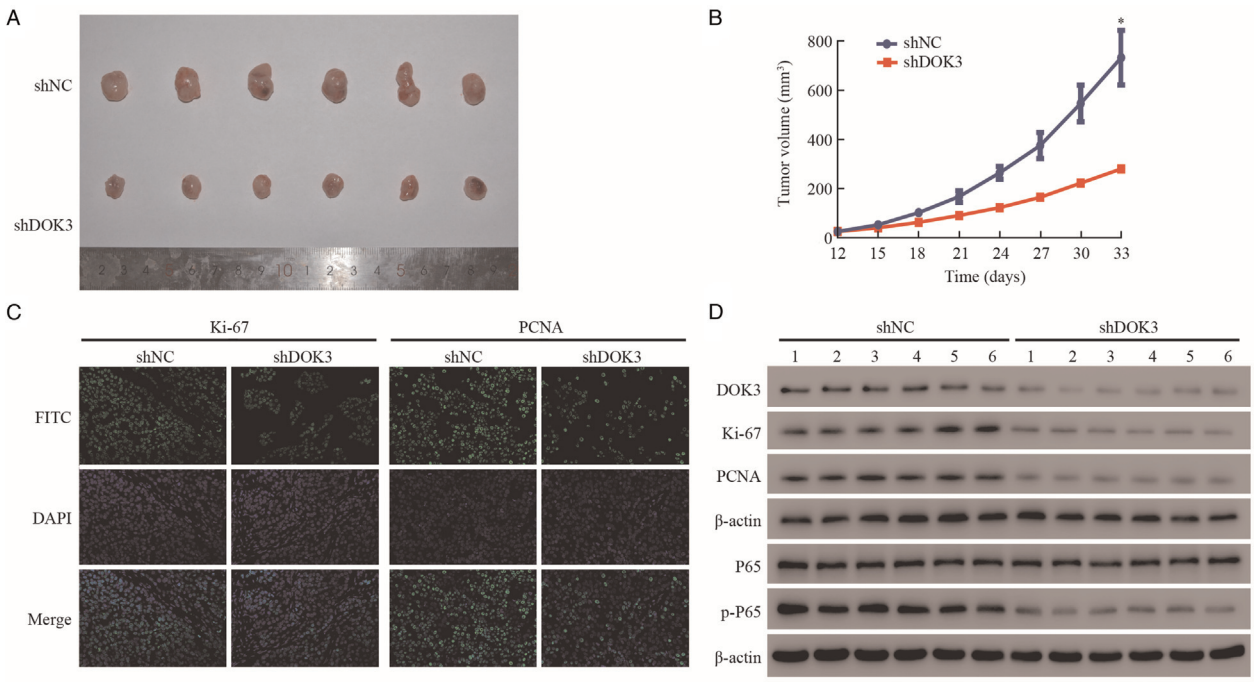

Figure 5: DOK3 knockdown suppresses tumor growth *in vivo*. (A) A xenograft nude mouse model was used to investigate the effect of DOK3 knockdown on tumor growth. 22Rv1 cells were transduced with shDOK3 or shNC lentivirus, and then injected subcutaneously into BALB/c nude mice. (B) Average tumor volume (mm^3) from day 12 after injection and measured after 3-week feed. (C) Representative images of fluorescence assessing expression levels of Ki67 and PCNA in xenograft tumor samples. (D) Protein levels of p-P65, P65, K-i67, and PCNA in tumor samples after transduction with shDOK3, using β-actin as the internal control, as determined by Western blotting analysis. Data represent mean ± SD and an unpaired *t*-test was used. $^{*}P < 0.0001$. DOK3: Downstream of kinase 3; SD: Standard deviation; shRNA: Short hairpin RNA; p-P65: Phosphorylated-p65; FITC: Fluorescein isothiocyanate; DAPI: 4',6-diamidino2-phenylindole; PCNA: Proliferating cell nuclear antigen.

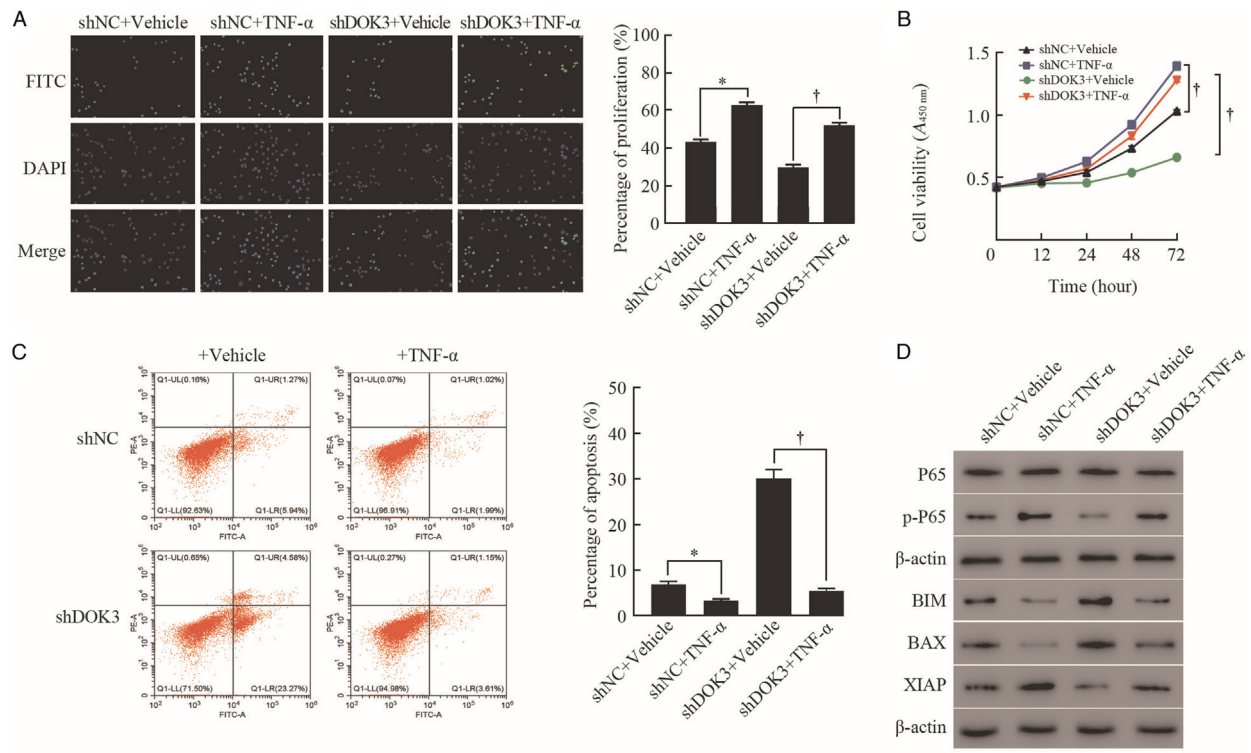

Figure 6: The effect of silencing DOK3 was suppressed via activating the NF-κB signaling pathway. (A, B) Proliferative capacity of 22Rv1 cell line measured by BrdU assay and CCK-8 assay. (C) Apoptosis rates of 22Rv1 cell line measured by flow cytometry analysis. (D) The expression of P65, p-P65, BIM, BAX, and XIAP was measured with the use of Western blotting assay. $^{*}P < 0.0001$, $^{\dagger}P < 0.001$. BrdU: Bromodeoxyuridine; CCK-8: Cell counting kit-8; DOK3: Downstream of kinase 3; shRNA: Short hairpin RNA; p-P65: Phosphorylated-p65; FITC: Fluorescein isothiocyanate; DAPI: 4',6-diamidino2-phenylindole.

PP1 and suppressed Card9 activity, further limiting signal transduction to NF-κB.[39] Under these circumstances, anti-fungal functions, such as phagocytosis and pro-inflammatory cytokine production, were inhibited.

There are several limitations of our study. First, the total p-P65 expression level was examined, but the origin of p-P65 was not distinguished; thus, it was not evaluated whether p-P65 entered the nuclei. Second, patient samples evaluated were substantially less than TCGA data; therefore, we failed to find a significant difference in correlation analysis between DOK3 level and pathological T stages. In addition, while we could verify that DOK3 acted as a tumor promoter through activating the NF-κB pathway, further exploration is needed to ascertain whether this occurs through direct interaction or a combination site.

In summary, we demonstrate that down-regulation of DOK3 decelerates PCa cell proliferation and tumor growth *in vivo* and *in vitro*. Therefore, DOK3 could potentially be an attractive therapeutic candidate for treating patients with PCa.

Acknowledgments

The authors acknowledge Ian Charles Tobias for reviewing the manuscript. We would also like to acknowledge all the staff members for their participation in study recruitment.

Funding

This study was supported by the National Key Research and Development Program of China (No. 2017YFC0908003).

Conflicts of interest

None.

References

1. Siegel RL, Miller KD, Fuchs HE, Jemal A. Cancer statistics, 2021. CA Cancer J Clin 2021;71:7–33. doi: 10.3322/caac.21654.
2. Sathianathen NJ, Konety BR, Crook J, Saad F, Lawrentschuk N. Landmarks in prostate cancer. Nat Rev Urol 2018;15:627–642. doi: 10.1038/s41585-018-0060-7.
3. Litwin MS, Tan HJ. The diagnosis and treatment of prostate cancer: a review. JAMA 2017;317:2532–2542. doi: 10.1001/jama.2017.7248.
4. Lee DJ, Mallin K, Graves AJ, Chang SS, Penson DF, Resnick MJ, *et al*. Recent changes in prostate cancer screening practices and epidemiology. J Urol 2017;198:1230–1240. doi: 10.1016/j.juro.2017.05.074.
5. Hamdy FC, Donovan JL, Lane JA, Mason M, Metcalfe C, Holding P, *et al*. 10-year outcomes after monitoring, surgery, or radiotherapy for localized prostate cancer. N Engl J Med 2016;375:1415–1424. doi: 10.1056/NEJMoa1606220.
6. Cai T, Santi R, Tamanini I, Galli IC, Perletti G, Bjerklund Johansen TE, *et al*. Current knowledge of the potential links between inflammation and prostate cancer. Int J Mol Sci 2019;20:3833. doi: 10.3390/ijms20153833.
7. de Bono JS, Guo C, Gurel B, De Marzo AM, Sfanos KS, Mani RS, *et al*. Prostate carcinogenesis: inflammatory storms. Nat Rev Cancer 2020;20:455–469. doi: 10.1038/s41568-020-0267-9.
8. Sfanos KS, Yegnasubramanian S, Nelson WG, De Marzo AM. The inflammatory microenvironment and microbiome in prostate cancer development. Nat Rev Urol 2018;15:11–24. doi: 10.1038/nrurol.2017.167.
9. Zhang K, Zhou S, Wang L, Wang J, Zou Q, Zhao W, *et al*. Current stem cell biomarkers and their functional mechanisms in prostate cancer. Int J Mol Sci 2016;17:1163. doi: 10.3390/ijms17071163.
10. Tsao T, Beretov J, Ni J, Bai X, Bucci J, Graham P, *et al*. Cancer stem cells in prostate cancer radioresistance. Cancer Lett 2019;465:94–104. doi: 10.1016/j.canlet.2019.08.020.
11. Shiao SL, Chu GCY, Chung LWK. Regulation of prostate cancer progression by the tumor microenvironment. Cancer Lett 2016;380:340–348. doi: 10.1016/j.canlet.2015.12.022.
12. Drake CG. Prostate cancer as a model for tumour immunotherapy. Nat Rev Immunol 2010;10:580–593. doi: 10.1038/nri2817.
13. Drake CG, Jaffee E, Pardoll DM. Mechanisms of immune evasion by tumors. Adv Immunol 2006;90:51–81. doi: 10.1016/S0065-2776(06)90002-9.
14. Mashima R, Hishida Y, Tezuka T, Yamanashi Y. The roles of Dok family adapters in immunoreceptor signaling. Immunol Rev 2009;232:273–285. doi: 10.1111/j.1600-065X.2009.00844.x.
15. Cong F, Yuan B, Goff SP. Characterization of a novel member of the DOK family that binds and modulates Abl signaling. Mol Cell Biol 1999;19:8314–8325. doi: 10.1128/MCB.19.12.8314.
16. Lemay S, Davidson D, Latour S, Veillette A. Dok-3, a novel adapter molecule involved in the negative regulation of immunoreceptor signaling. Mol Cell Biol 2000;20:2743–2754. doi: 10.1128/MCB.20.8.2743-2754.2000.
17. Manno B, Oellerich T, Schnyder T, Corso J, Lösing M, Neumann K, *et al*. The Dok-3/Grb2 adaptor module promotes inducible association of the lipid phosphatase SHIP with the BCR in a coreceptor-independent manner. Eur J Immunol 2016;46:2520–2530. doi: 10.1002/eji.201646431.
18. Ou X, Xu S, Li YF, Lam KP. Adaptor protein DOK3 promotes plasma cell differentiation by regulating the expression of programmed cell death 1 ligands. Proc Natl Acad Sci U S A 2014;111:11431–11436. doi: 10.1073/pnas.1400539111.
19. Ng CH, Xu S, Lam KP. Dok-3 plays a nonredundant role in negative regulation of B-cell activation. Blood 2007;110:259–266. doi: 10.1182/blood-2006-10-055194.
20. Stork B, Neumann K, Goldbeck I, Alers S, Kähne T, Naumann M, *et al*. Subcellular localization of Grb2 by the adaptor protein Dok-3 restricts the intensity of Ca2+ signaling in B cells. EMBO J 2007;26:1140–1149. doi: 10.1038/sj.emboj.7601557.
21. Kim SSY, Lee KG, Chin CS, Ng SK, Pereira NA, Xu S, *et al*. DOK3 is required for IFN-beta production by enabling TRAF3/TBK1 complex formation and IRF3 activation. J Immunol 2014;193:840–848. doi: 10.4049/jimmunol.1301601.
22. Peng Q, Long CL, Malhotra S, Humphrey MB. A physical interaction between the adaptor proteins DOK3 and DAP12 is required to inhibit lipopolysaccharide signaling in macrophages. Sci Signal 2013;6:ra72. doi: 10.1126/scisignal.2003801.
23. Liu N, Liu X, Li X, Duan K, Deng Y, Yu X, *et al*. DOK3 degradation is required for the development of LPS-induced ARDS in mice. Curr Gene Ther 2016;16:256–262. doi: 10.2174/1566523216666161103142342.
24. Liu X, Chen F, Li W. Elevated expression of DOK3 indicates high suppressive immune cell infiltration and unfavorable prognosis of gliomas. Int Immunopharmacol 2020;83:106400. doi: 10.1016/j.intimp.2020.106400.
25. Berger AH, Niki M, Morotti A, Taylor BS, Socci ND, Viale A, *et al*. Identification of DOK genes as lung tumor suppressors. Nat Genet 2010;42:216–223. doi: 10.1038/ng.527.
26. Schnyder T, Castello A, Feest C, Harwood NE, Oellerich T, Urlaub H, *et al*. B cell receptor-mediated antigen gathering requires ubiquitin ligase Cbl and adaptors Grb2 and Dok-3 to recruit dynein to the signaling microcluster. Immunity 2011;34:905–918. doi: 10.1016/j.immuni.2011.06.001.
27. Peng Q, O'Loughlin JL, Humphrey MB. DOK3 negatively regulates LPS responses and endotoxin tolerance. PLoS One 2012;7:e39967. doi: 10.1371/journal.pone.0039967.
28. Liu N, Tang B, Wei P, Sun W, Wang S, Peng Q. TRAF6-mediated degradation of DOK3 is required for production of IL-6 and TNFalpha in TLR9 signaling. Mol Immunol 2015;68 (2 Pt C):699–705. doi: 10.1016/j.molimm.2015.10.021.
29. Mashima R, Arimura S, Kajikawa S, Oda H, Nakae S, Yamanashi Y. Dok adaptors play anti-inflammatory roles in pulmonary homeostasis. Genes Cells 2013;18:56–65. doi: 10.1111/gtc.12016.

30. Cai X, Xing J, Long CL, Peng Q, Humphrey MB. DOK3 modulates bone remodeling by negatively regulating osteoclastogenesis and positively regulating osteoblastogenesis. J Bone Miner Res 2017;32:2207–2218. doi: 10.1002/jbmr.3205.
31. Sun SC. The non-canonical NF-kappaB pathway in immunity and inflammation. Nat Rev Immunol 2017;17:545–558. doi: 10.1038/nri.2017.52.
32. Beg AA, Baltimore D. An essential role for NF-kappaB in preventing TNF-alpha-induced cell death. Science 1996;274:782–784. doi: 10.1126/science.274.5288.782.
33. Liu ZG, Hsu H, Goeddel DV, Karin M. Dissection of TNF receptor 1 effector functions: JNK activation is not linked to apoptosis while NF-kappaB activation prevents cell death. Cell 1996;87:565–576. doi: 10.1016/s0092-8674(00)81375-6.
34. Van Antwerp DJ, Martin SJ, Kafri T, Green DR, Verma IM. Suppression of TNF-alpha-induced apoptosis by NF-kappaB. Science 1996;274:787–789. doi: 10.1126/science.274.5288.787.
35. Wang CY, Mayo MW, Baldwin AS Jr. TNF- and cancer therapy-induced apoptosis: potentiation by inhibition of NF-kappaB. Science 1996;274:784–787. doi: 10.1126/science.274.5288.784.
36. Joyce D, Albanese C, Steer J, Fu M, Bouzahzah B, Pestell RG. NF-kappaB and cell-cycle regulation: the cyclin connection. Cytokine Growth Factor Rev 2001;12:73–90. doi: 10.1016/s1359-6101(00)00018-6.
37. Karin M, Cao Y, Greten FR, Li ZW. NF-kappaB in cancer: from innocent bystander to major culprit. Nat Rev Cancer 2002;2:301–310. doi: 10.1038/nrc780.
38. DiDonato JA, Mercurio F, Karin M. NF-kappaB and the link between inflammation and cancer. Immunol Rev 2012;246:379–400. doi: 10.1111/j.1600-065X.2012.01099.x.
39. Loh JT, Xu S, Huo JX, Kim SS, Wang Y, Lam KP. Dok3-protein phosphatase 1 interaction attenuates Card9 signaling and neutrophil-dependent antifungal immunity. J Clin Invest 2019;129:2717–2729. doi: 10.1172/JCI126341.

How to cite this article: Jin K, Qiu S, Chen B, Zhang Z, Zhang C, Zhou X, Yang L, Ai J, Wei Q. DOK3 promotes proliferation and inhibits apoptosis of prostate cancer via the NF-κB signaling pathway. Chin Med J 2023;136:423–432. doi: 10.1097/CM9.0000000000002251